Profilin1 regulates PI(3,4)P_2 and lamellipodin accumulation at the leading edge thus influencing motility of MDA-MB-231 cells

Yong Ho Bae[a], Zhijie Ding[a,1], Tuhin Das[a,1], Alan Wells[a,b,c], Frank Gertler[d], and Partha Roy[a,b,2]

[a]Department of Bioengineering, University of Pittsburgh, Pittsburgh, PA 15219; [b]Department of Pathology, University of Pittsburgh, Pittsburgh, PA 15261; [c]Pittsburgh Veterans Afffairs Medical Center, Pittsburgh, PA 15240; and [d]Department of Biology and Koch Center for Cancer Research, Massachusetts Institute of Technology, Cambridge, MA 02139

Edited* by Thomas D. Pollard, Yale University, New Haven, CT, and approved November 4, 2010 (received for review February 25, 2010)

Profilin1, a ubiquitously expressed actin-binding protein, plays a critical role in cell migration through actin cytoskeletal regulation. Given the traditional view of profilin1 as a promigratory molecule, it is difficult to reconcile observations that profilin1 is down-regulated in various invasive adenocarcinomas and that reduced profilin1 expression actually confers increased motility to certain adenocarcinoma cells. In this study, we show that profilin1 negatively regulates lamellipodin targeting to the leading edge in MDA-MB-231 breast cancer cells and normal cells; profilin1 depletion increases lamellipodin concentration at the lamellipodial tip (where it binds Ena/VASP), and this mediates the hypermotility. We report that the molecular mechanism underlying profilin1's modulation of lamellipodin localization relates to phosphoinositide control. Specifically, we show that phosphoinositide binding of profilin1 inhibits the motility of MDA-MB-231 cells by negatively regulating PI(3,4)P_2 at the membrane and thereby limiting recruitment of lamellipodin [a PI(3,4)P_2-binding protein] and Ena/VASP to the leading edge. In summary, this study uncovers a unique biological consequence of profilin1-phosphoinositide interaction, thus providing direct evidence of profilin1's regulation of cell migration independent of its actin-related activity.

The ubiquitously expressed cytoskeleton-modulating protein profilin1 influences multiple processes involved in cell motility, making it a challenge to elucidate the exact molecular mechanism that controls migration. At least one major function of profilin1 is to regulate actin polymerization. Profilin1 regenerates actin monomers from disassembling filament networks by facilitating the exchange of ATP for ADP on G-actin. By further inhibiting spontaneous nucleation of G-actin, profilin1 causes an accumulation of profilin1/ATP-G-actin pool available for polymerization. Because profilin1 also has an affinity for poly-L-proline sequences, it binds to almost all major actin nucleating and F-actin elongating proteins that contain proline-rich domains [e.g., N-WASP (neuronal Wiskott–Aldrich syndrome protein), Ena (enabled)/VASP (vasodilator stimulated phosphoprotein), and formins], and this allows profilin1-mediated recruitment of ATP-G-actin to these proteins, enhancing actin polymerization (1, 2). In addition, profilin1 binds to plasma membrane presumably through its interactions with various phosphoinositides (3). Profilin1 binds to phosphatidylinositol-4,5-bisphosphate [PI(4,5)P_2], phosphatidylinositol-3,4-bisphosphate [PI(3,4)P_2], and phosphatidylinositol-3,4,5-triphosphate [PI(3,4,5)P_3]), at least in vitro (4). Based on PI(4,5)P_2 binding, it has been proposed that the phosphoinositide binding site of profilin1 overlaps with its actin-binding site (5), and to some extent spans a second region neighboring the polyproline binding site (6). This has prompted speculation that the major role of phosphoinositide binding of profilin1 would be to inhibit its interaction with actin by sequestering it at the plasma membrane (5). The interactions of profilin1 with actin and actin regulatory proteins have been studied fairly extensively in the context of cytoskeletal regulation. However, relatively few studies have focused on the profilin1/phosphoinositide interaction, and these studies were mostly performed in vitro using pure protein-phospholipid mixtures (4, 5, 7). Therefore, the physiological role of profilin1's interaction with phosphoinositides has remained unclear, as has the potential role of the phosphoinositide interaction in pathophysiology.

We previously demonstrated that profilin1's interactions with actin and polyproline ligands are critical for vascular endothelial cell motility (8, 9). Seemingly contrary to the conventional model of profilin1 promoting migration, invasive mammary carcinoma cells present down-regulated profilin1 expression (10). Our previous studies showed that silencing profilin1 expression leads to faster motility of both normal human mammary epithelial cells (HMEC) and metastatic MDA-MB-231 (MDA-231) breast cancer cell line; conversely, even a moderate overexpression of profilin1 dramatically suppresses motility of MDA-231 and BT474 breast cancer cell lines (11–13). This paradoxical effect of profilin1 in cell migration has also been reported for hepatocarcinoma cells where profilin1 expression also appears down-regulated (14). These findings suggest that profilin1's role in cell migration is complex and contextual. Given the traditionally conceived promigratory function of profilin1 mediated mainly through its interactions with actin and actin regulatory proteins, the existing literature cannot explain how loss of profilin1 expression augments carcinoma cell motility. Here, we discuss a unique mechanism that links the phosphoinositide binding of profilin1 to the inhibition of breast cancer cell motility. This involves negative regulation of PI(3,4)P_2 availability with subsequent reduction in targeting of the PI(3,4)P_2-binding protein lamellipodin to the leading edge.

Results

Profilin1 Inhibits MDA-MB-231 Cell Motility Predominantly Through Its Phosphoinositide Interaction. To investigate how reduced profilin1 level increases breast cancer cell motility, we first asked which among the three major ligand interactions of profilin1 (actin, polyproline, or phosphoinositide) is predominantly responsible for the inhibition of cell migration. Our overall experimental strategy involved rescue of profilin1-depleted MDA-231 cells by either WT or various ligand-binding-deficient mutants of profilin1. Binding sites for actin and polyproline within profilin1 have been mapped; however, the exact location of profilin1's

Author contributions: Y.H.B., Z.D., A.W., and P.R. designed research; Y.H.B., Z.D., T.D., and P.R. performed research; Y.H.B., Z.D., F.G., and P.R. contributed new reagents/analytic tools; Y.H.B. analyzed data; and Y.H.B., A.W., F.G., and P.R. wrote the paper.

The authors declare no conflict of interest.

*This Direct Submission article had a prearranged editor.

[1]Z.D. and T.D. contributed equally to this work.

[2]To whom correspondence should be addressed. E-mail: par19@pitt.edu.

This article contains supporting information online at www.pnas.org/lookup/suppl/doi:10.1073/pnas.1002309107/-/DCSupplemental.

CELL BIOLOGY

phosphoinositide binding is much less certain. We selected three previously characterized point-mutants (H119E, H133S, and R88L) of profilin1 to perturb its interactions with various ligands. Table S1 summarizes how each of these mutations affects various ligand interactions of profilin1, as determined by quantitative and nonquantitative binding assays in previous studies [only phosphoinositide binding of H119E-profilin1 was not specifically tested previously; we qualitatively confirmed that H119E substitution does not impair profilin1's phosphoinositide binding (Fig. S1), and this is consistent with a previously reported finding for the analogous H119D mutant (15)]. In summary, H119E and H133S substitutions selectively abolish profilin1's interaction with actin (25-fold lower binding than WT) and polyproline ligands (50-fold lower binding than WT), respectively (16). R88L substitution not only causes a major defect in phosphoinositide binding of profilin1 [its affinity for $PI(4,5)P_2$ is threefold lower than WT] (15, 17), but also severely impairs profilin1's ability to inhibit actin polymerization and exchange nucleotide on actin in vitro (15). This implies that R88L-profilin1 is also defective in actin binding (this is true for all other phosphoinositide mutants of profilin1 identified to date and results from likely overlap between actin and phosphoinositide binding sites within profilin1).

For rescue experiments, we stably expressed either WT or the aforementioned mutants of profilin1 as GFP-tagged proteins in MDA-231 cells. We adopted GFP tagging to monitor the expression levels of rescue profilin1 constructs in our cell lines. Even though N-terminal fusion of GFP with a flexible linker introduced between the GFP and profilin1 moieties, as also done in our case, reduces its polyproline binding to a certain extent (as judged by a ~50% reduction in VASP binding in vitro (18); note that actin and phosphoinositide binding are not significantly affected), GFP-profilin1 is a valid rescue construct based on the following functional evidence in cells. First, GFP-profilin1 localizes at the regions of high actin dynamics (leading edge, ruffles) similar to endogenous profilin1 in cells (18), thus GFP-profilin1 most likely interacts with the binding partners of profilin1 that regulate actin dynamics in cells [we have confirmed GFP-profilin1's interaction with, at least, VASP in cells (19)]. Second, we showed that GFP-profilin1 can completely rescue protrusion/migration defects of profilin1-depleted endothelial cells (8). Third, GFP-tagged profilin1 mutants defective for actin and polyproline binding (H119E and H133S) inhibit pathogen-induced actin polymerization in host cells by dominant negative action, as expected (20).

To mimic rescue, we selectively depleted endogenous profilin1 in the various stable cell lines by profilin1-siRNA transfection; all GFP-tagged profilin1 constructs were rendered resistant to profilin1-siRNA by introducing additional silent mutations in the siRNA targeting region. As a control, our previously generated stable GFP expressers (12) were transfected with either nontargeting control or profilin1-siRNA. Fig. 1*A* shows similar expression levels of various rescue profilin1 constructs between the different sublines in a near absence of endogenous profilin1 background. The expression level of exogenous profilin1 was estimated to be 70–80% of that of endogenous profilin1 (Fig. 1*B*). GFP-profilin1 was found to be more abundant in the cytosol than in the membrane (Fig. 1*C*), agreeing with a previous report on endogenous profilin1 distribution (3). As expected, the membrane content of R88L-profilin1 defective in phosphoinositide binding was almost negligible compared with the other three variants of profilin1 (Fig. 1*D*).

Time-lapse imaging revealed that MDA-231 cells depleted of profilin1 migrated twice as fast as controls, as shown previously (11). Expression of GFP-profilin1 suppressed the hypermotile phenotype, further confirming functionality of GFP-profilin1 in MDA-231 cells. Among the mutants, only the one with weaker phosphoinositide binding (R88L-profilin1) was unable to rescue the hypermotility of profilin1 knockdown cells (Fig. 1*E*). Although R88L substitution causes a concomitant defect in actin

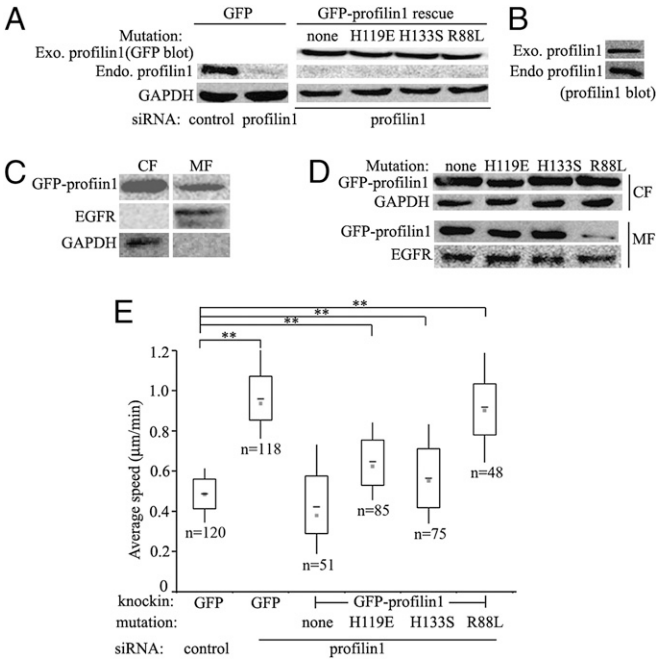

Fig. 1. Rescue of profilin1-depleted MDA-231 cells with GFP-tagged profilin1 constructs, and the resulting effects on cell motility. (*A*) Total lysates from siRNA-transfected (as indicated) MDA-231 sublines were immunoblotted with anti-GFP, anti-profilin1, and anti-GAPDH (loading control) antibodies. (*B*) Total lysate from control-siRNA treated GFP-profilin1 expressers was immunoblotted with anti-profilin1 antibody (Exo, exogenous; Endo, endogenous). (*C*) Fractionated lysates (CF, cytoplasmic fraction; MF, membrane fraction) of GFP-profilin1 expressers were immunoblotted with anti-GFP, anti-EGFR (marker for MF), and anti-GAPDH (marker for CF) antibodies. (*D*) Fractionated lysates from MDA-231 cells expressing indicated profilin1 constructs were immunoblotted with anti-GFP, anti-EGFR (loading control for MF) and anti-GAPDH (loading control for CF) antibodies. Note that the exposure time for MF blot was much higher than the CF blot to reveal the weak MF band for R88L-profilin1. Nuclear content of profilin1 (strongest for H119E-profilin1 mutant) was not analyzed here. (*E*) A box and whisker plot that summarizes the average speed of various rescue sublines. n, no. of cells pooled from three experiments. $^{**}P < 0.01$.

binding of profilin1, given that H119E-profilin1 (a mutant that is severely defective in actin binding but has normal phosphoinositide binding) was able to substantially reduce the speed of profilin1 knockdown cells, hypermotility of profilin1-deficient MDA-231 cells most likely arises from loss of profilin1's phosphoinositide binding rather than actin monomer binding activity. We earlier showed that profilin1 depletion in MDA-231 cells results in slower but longer-lived membrane protrusion, thereby increasing the net protrusion over time (11). Here we used the term "net lamellipodial extension," a metric that reflects the overall length of membrane extension over time but not the individual components of lamellipodial dynamics that are involved in motility (lamellipodial protrusion speed, protrusion duration, withdrawal length and duration). All groups of cells analyzed here formed lamellipodia with normal morphology (Fig. S2*A*); however, kymography analyses of membrane dynamics showed that only the mutant with impaired phosphoinositide binding (R88L-profilin1) failed to correct the abnormal net lamellipodial extension of profilin1-depleted cells (Fig. S2 *B* and *C*). Because cells rescued with WT and R88L mutant of profilin1 showed similar levels of filamentous and total actin (Fig. S2 *D* and *E*), the large net lamellipodial extension of R88L-profilin1 expressers could be due to possible changes in F-actin dynamics and/or protrusion/adhesion coupling at the leading edge resulting from the loss of profilin1/phosphoinositide binding. In summary, our

data suggest that profilin1 inhibits MDA-231 cell migration predominantly through its phosphoinositide interaction, and that actin binding does not play a major role in the effect of profilin1 on the speed of this cell line.

Profilin1 Inhibits MDA-MB-231 Cell Motility by Attenuating Lamellipodin Targeting to the Leading Edge. Ena/VASP proteins play an important role in regulating F-actin elongation and membrane protrusion at the leading edge, and we previously showed that profilin1 knockdown enhances net lamellipodial extension and overall motility of MDA-231 cells through increased Ena/VASP accumulation at the leading edge (11). Consistent with our motility and kymograph data, rescue experiments showed that only the profilin1 mutant with reduced phosphoinositide binding (R88L-profilin1) failed to change the VASP-rich lamellipodial rim in profilin1 knockdown cells (Fig. 2*A*). Thus, phosphoinositide interaction of profilin1 likely inhibits Ena/VASP targeting to the leading edge.

Lamellipodin, a phosphoinositide binding protein, was previously shown to play an important role in recruiting Ena/VASP to the leading edge in fibroblasts and melanoma cells (note that lamellipodin targets to the leading edge independently of Ena/VASP) (21, 22). Lamellipodin depletion by siRNA markedly reduced VASP accumulation at the leading edge in profilin1 knockdown MDA-231 cells (Fig. 2 *B* and *C*), thus confirming a critical role of lamellipodin in targeting VASP to the lamellipodial tip in our breast cancer cell line. Consistent with this interpretation, we found that profilin1 knockdown did not affect the expression of lamellipodin (Fig. 2*D*) but caused a fourfold increase in its accumulation at the leading edge (Fig. 2*E* and Fig. S3). Conversely, cells stably overexpressing (~twofold) GFP-profilin1 presented a ~25% reduction in lamellipodin distribution at the leading edge compared with GFP controls (Fig. 2*E* and Fig. S3). Even normal HMEC and human umbilical vein endothelial cells (HUVEC) exhibited similar lamellipodin enrichment at the leading edge upon profilin1 depletion (Fig. S4), suggesting a generality of profilin1-dependent regulation of lamellipodin localization in cells. Interestingly, though HMEC are similarly hypermotile upon profilin1 depletion (11), HUVEC actually become hypomotile (9). Next, rescue experiments showed that only the profilin1 mutant with impaired phosphoinositide binding (R88L-profilin1) failed to correct the increased accumulation of lamellipodin at the leading edge in profilin1-depleted MDA-231 cells (Fig. 2*F*). Phenotypes of R88L-profilin1 expressers (i.e., strong lamellipodin accumulation at the leading edge, hypermotility) were abrogated when cells were treated with control siRNA (mimics overexpression of the mutant; Fig. S5). Because endogenous profilin1 presumably still interacted with plasma membrane when R88L-profilin1 is overexpressed, these data support a model of profilin1's negative regulation of lamellipodin localization via phosphoinositide interaction.

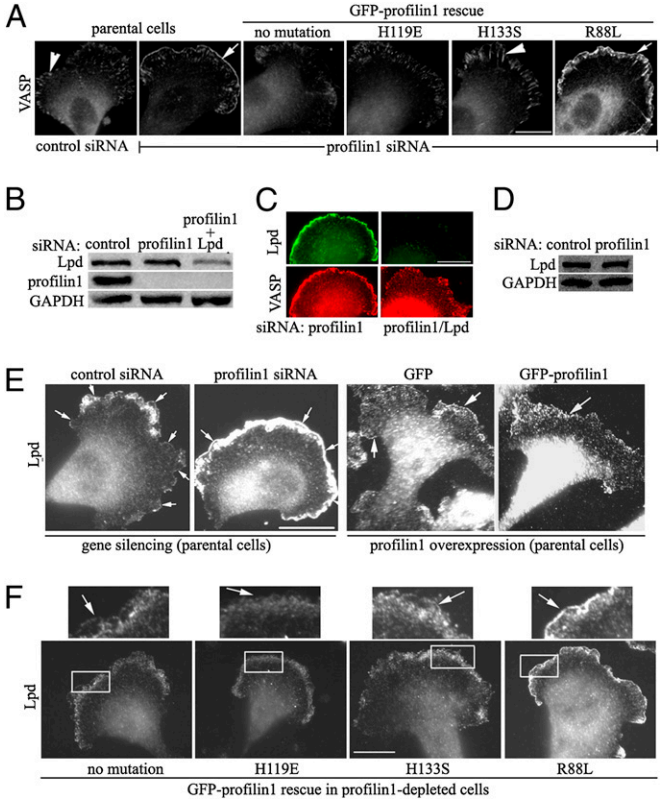

Fig. 2. Profilin1-dependent regulation of VASP and Lpd localization in MDA-231 cells. (*A*) Fluorescence micrographs of control and profilin1 knockdown (without or with rescued by the indicated constructs) cells stained with anti-VASP antibody. Arrows and arrowheads show VASP localization at the leading edge and focal adhesions, respectively. (*B*) Lysates from siRNA-transfected (as 4indicated) cells were immunoblotted with anti-Lpd, anti-profilin1, and anti-GAPDH (loading control) antibodies. (*C*) Fluorescence micrographs of siRNA-transfected (as indicated) cells costained with anti-VASP and anti-Lpd antibodies. (*D*) Total lysates from siRNA-transfected (as indicated) cells were immunoblotted with anti-Lpd and anti-GAPDH (loading control) antibodies. (*E* and *F*) Fluorescence micrographs of cells stained with anti-Lpd antibody. In *E*, cells were either treated with siRNAs (control/profilin1) or stably transfected with plasmids (GFP/GFP-profilin1). In *F*, cells were treated with profilin1 siRNA and rescued with the indicated profilin1 constructs. Magnified insets and arrows show regions of interest at the leading edge. (Scale bar, 20 μm.)

We next asked whether lamellipodin plays a role in hypermotility of profilin1-depleted MDA-231 cells. In the presence of profilin1, lamellipodin knockdown caused a slight narrowing of lamellipod (suggesting mild protrusion defect) in cells plated on uncoated tissue-culture substrate. On collagen I-coated substrate (our usual condition for motility assays), lamellipodia morphology and the overall speed of MDA-231 cells were not affected by lamellipodin knockdown (Fig. 3*A* and Fig. S6*A*). However, when profilin1 expression was silenced, lamellipodin knockdown led to a major defect in spreading (Fig. S6*A*), prominent reduction in the F-actin content at the leading edge (Fig. S6*B*), much lower net membrane extension (Fig. S6*C*), and a twofold reduction in the overall cell speed (Fig. 3*A*). Profilin1-depleted HMEC also migrated substantially slower in response to lamellipodin knockdown (Fig. S7). These data show that lamellipodin mediates hypermotility of profilin1-depleted MDA-231 cells.

Finally, consistent with our interpretation of profilin1's negative regulation of lamellipodin/VASP targeting to the leading edge through phosphoinositide interaction, hypermotility of R88L-profilin1 rescue expressers was also suppressed when either lamellipodin was knocked down or downstream Ena/VASP proteins were displaced from their normal cellular locations by transiently expressing FP4-mito (a construct that binds to and displaces all detectable Ena/VASP to the mitochondria in various cells, including MDA-231 cells; refs. 11 and 23) (Fig. 3*B*). The slightly more robust effect of Ena/VASP mislocalization than lamellipodin depletion on the motility of R88L-profilin1 expressers (3.2-fold vs. twofold inhibition) likely arises from incomplete knockdown of lamellipodin expression; Fig. 3*C*). In summary, our data suggest that phosphoinositide binding of profilin1 inhibits MDA-231 cell motility through limiting lamellipodin accumulation and in turn Ena/VASP recruitment to the leading edge.

Profilin1 Inhibits PI(3,4)P_2 Presentation at the Leading Edge. Lamellipodin contains a PH (pleckstrin homology) domain that binds PI(3,4)P_2 with much higher affinity than any other tested 3′-phosphorylated phosphoinositides (D3-phosphoinositides) such

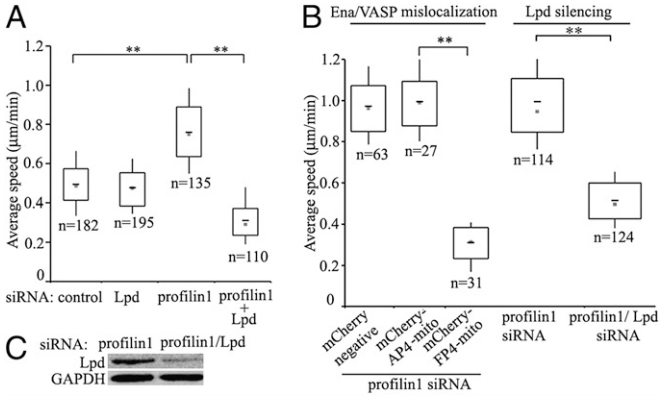

Fig. 3. Effect of Lpd knockdown on MDA-231 cell motility. (*A*) A box and whisker plot representing the average speed of MDA-231 cells following treatment with the indicated siRNAs. (*B*) A box and whisker plot summarizing the effects of Ena/VASP mislocalization and Lpd knockdown on the average speed of R88L-profilin1 expressers under endogenous profilin1-depleted condition. Ena/VASP was mislocalized to mitochondria by expressing mCherry-FP4-mito [cells, untransfected (mCherry negative) and/or expressing mCherry-AP4-mito (a mitochondrial targeting construct that does not bind Ena/VASP), served as controls]. n, no. of analyzed cells pooled from three experiments. $^{**}P < 0.01$. (*C*) Lysates of R88L-profilin1 expressers (transfected with the indicated siRNAs) were immunoblotted with anti-Lpd and anti-GAPDH (loading control) antibodies.

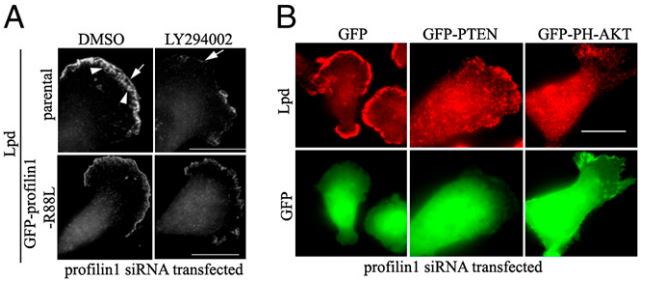

Fig. 4. Effect of reducing D3-phosphoinositide availability on Lpd localization in MDA-231 cells. Fluorescence micrographs of profilin1 knockdown cells (without or with R88L-profilin1 rescue) stained with anti-Lpd antibody (*A* and *B Upper*). In *A*, cells were pretreated for 30 min with either LY294002 or DMSO (control) before 30 min of PDGF stimulation. In *B*, cells were transiently transfected with either GFP- (control), GFP-PTEN-, or GFP-PH-AKT-encoding plasmid (transfected cells were identified by GFP fluorescence; *Lower*). Arrows and arrowheads show Lpd localization at the leading edge and membrane ruffles, respectively. (Scale bar, 20 μm.)

as PI3P or PI(3,4,5)P_3 (21). According to a recent report (24), PI(3,4)P_2 is generated at the sites of lamellipodin recruitment in cells. Thus PI(3,4)P_2 appears to be a key phosphoinositide for membrane docking of lamellipodin. Activation of receptor tyrosine kinases (RTKs) such as EGFR (EGF receptor) and PDGFR (PDGF receptor) lead to PI3 kinase (PI3K)-mediated generation of D3-phosphoinositides, including PI(3,4,5)P_3 and PI(3,4)P_2 [the latter mostly through PI(3,4,5)P_3 dephosphorylation by 5′-phosphatases]. Consistent with this, PDGF stimulation has been shown to recruit lamellipodin or even the isolated PH domain of lamellipodin to the leading edge and the tips of dorsal ruffles (21, 22). We found that PI3K inhibition by LY294002 dramatically inhibits lamellipodin accumulation at the leading edge in profilin1 knockdown MDA-231 cells (with or without rescue by R88L-profilin1) under PDGF-stimulated condition (Fig. 4*A*). Similar changes with regard to lamellipodin localization were seen when profilin1 knockdown cells were subjected to overexpression of either GFP-PTEN (phosphatase and tensin homolog deleted on chromosome 10—a phosphatase that reduces the levels of D3-phosphoinositides) or GFP-PH-AKT (a reporter that binds to D3-phosphoinositides and therefore should competitively inhibit D3-phosphoinositide/ligand interactions; Fig. 4*B*). These findings directly demonstrated that membrane availability of D3-phosphoinositides is critical for lamellipodin recruitment to the leading edge.

Based on the above findings, we speculated that profilin1 may play a role in regulating PI(3,4)P_2. Thus, we compared PI(3,4)P_2 distribution at the leading edge between control and profilin1 knockdown cells under basal (serum-starved) vs. growth-factor (EGF, PDGF) stimulated conditions by immunofluoresence analysis. We chose to investigate PI(3,4)P_2 status in response to specific growth-factor stimulation for two reasons. First, PI(3,4)P_2 is not an abundant phosphoinositide, and the most robust increase in PI(3,4)P_2 synthesis occurs after acute stimulation of EGF/PDGF, thereby facilitating detection by immunostaining using commercially available antibodies. Second, signaling pathways can be studied in a more defined manner in a setting of single growth-factor treatment. EGF signaling, in particular, plays a key role in breast cancer cell migration/invasion in vitro and in vivo (25). Treatment with EGF or PDGF stimulated PI(3,4)P_2 production in both control and profilin1 knockdown MDA-231 cells, but the anti-PI(3,4)P_2 staining was twofold higher at the leading edge of profilin1 knockdown cells (Fig. 5 *A* and *B*). EGF-induced PI(3,4)P_2 accumulation at the leading edge in profilin1 knockdown cells was dramatically reduced (by ∼80%) by profilin1 rescue, but reexpression of R88L-profilin1 (with lower affinity for phosphoinositides) reduced the PI(3,4)P_2 signal by only 30% (Fig. 5 *C* and *D*); this 30% difference is not surprising, because the R88L mutation does not abolish the profilin1/phosphoinositide interaction completely. These data suggest that phosphoinositide interaction of profilin1 could inhibit PI(3,4)P_2 presentation at the leading edge in MDA-231 cells. Control experiments showed profilin1 depletion did not alter RTK activation. Essentially, EGFR activation (judged by Y1164 phosphorylation of EGFR), the overall expression level of EGFR, EGF-dependent phosphorylation of AKT (a downstream signaling involving PI3K activity; Fig. 5*E*), expression of PDGFRβ, or tyrosine phosphorylation of PDGFR (correlates with its activation; Fig. S8) in MDA-231 cells were unaffected by profilin1 knockdown. Thus it is likely that profilin1 alters PI(3,4)P_2 level through perturbing phosphoinositide turnover.

Discussion

A context-dependent role for profilin1 in cell migration has become evident based on the cell type-dependent effects of profilin1 depletion on whole-cell motility. Whereas certain cell types, such as HUVEC, show impaired motility upon loss of profilin1, the opposite occurs in adenocarcinoma lines (breast, hepatic) and even in some normal cells such as HMEC. The prevailing model for profilin1 function in which interactions with actin and polyproline ligands facilitate membrane protrusion during cell migration cannot explain the hypermotile response of breast cancer cells and HMEC enabled in the absence of profilin1. We here describe a regulatory pathway that limits breast cancer cell motility by linking the phosphoinositide interaction of profilin1 to reduced availability of PI(3,4)P_2 and concomitant reduced lamellipodin/Ena-VASP targeting to the leading edge. This report shows that profilin1 regulates cell migration independently of its commonly studied actin-binding activity, revealing an important aspect of the physiological consequence of profilin1/phosphoinositide interaction.

Our interpretation that phenotypes of profilin1 knockdown cells (i.e., hypermotility, increased VASP/lamellipodin accumulation at the leading edge) are most likely related to loss of profilin1/phosphoinositide interaction was based on rescuing

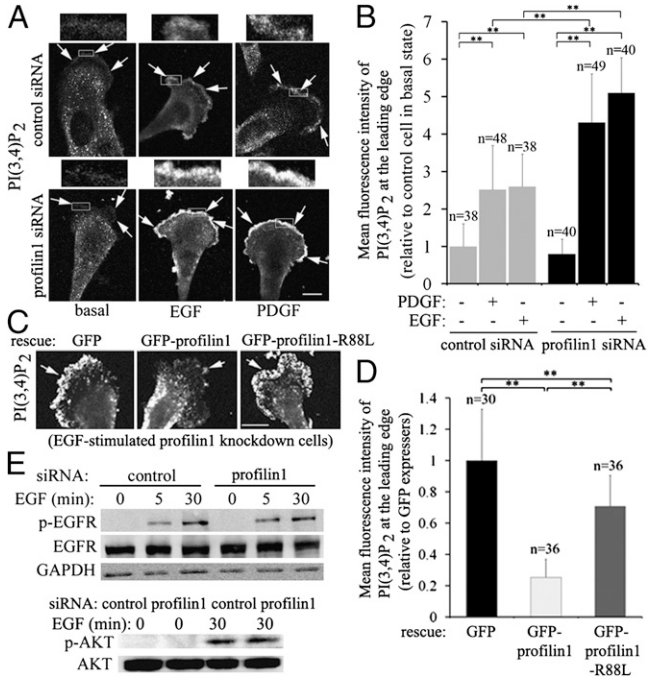

Fig. 5. Profilin1's effect on $PI(3,4)P_2$ concentration at the leading edge in MDA-231 cells. (*A*) Fluorescence micrographs of MDA-231 cells stained with $PI(3,4)P_2$ antibody. (*Upper*) Cells treated with control siRNA. (*Lower*) Cells treated with profilin1 siRNA. Treatments: column 1, none (serum starved); column 2, 100 ng/mL EGF for 30 min; column 3, 100 ng/mL PDGF for 30 min. (*B*) Quantitative measurements of the fluorescence at the leading edges of cells from the experiment in *A*. (*C*) Fluorescence micrographs of profilin1-siRNA transfected MDA-231 cells (without or with rescue by profilin1 constructs) stained with $PI(3,4)P_2$ antibody. (*Left*) Cell expressed GFP (no rescue). (*Center* and *Right*) Cells expressed GFP-profilin1 and GFP-profilin1-R88L, respectively. Cells in all three groups were serum starved and then stimulated with 100 ng/mL EGF for 30 min before performing $PI(3,4)P_2$ staining. (*D*) Quantitative measurements of the fluorescence at the leading edges of cells from the experiment in *C*. (*E*) Total lysates from control and profilin1 knockdown cells were immunoblotted with anti-EGFR, anti-phospho-EGFR, anti-GAPDH (loading control), anti-phospho-AKT, and anti-AKT (loading control) antibodies. In immunostaining images, magnified insets and arrows show regions of interest at the leading edge. $*P < 0.01$. (Scale bar, 20 μm.)

ability of previously described point mutants of profilin1. It is difficult to predict how in vitro binding data of profilin1 mutants (as reported in the literature) translate to their in vivo interactions. Particularly, there is the issue of extent of changed affinity in vitro translating into cellular behaviors. For instance, a previous work on yeast showed that profilin1 mutants must have dramatically altered interactions to elicit changes in cellular responses (26). We have tried to account for this issue. First, negligible membrane content of R88L-profilin1 compared with other rescue constructs in MDA-231 cells implied a major impairment in membrane interaction of R88L-profilin1 in vivo. Membrane contents of actin (H119E) and polyproline (H133S) mutants of profilin1 were comparable to that of WT rescue construct; thus these two mutants likely maintained normal membrane phosphoinositide interaction in cells. Second, our previous studies showed that in vivo interactions of H119E and H133S mutants with actin and polyproline ligands, respectively, are practically undetectable by coimmunoprecipitation and/or FRET assays (12, 19). Therefore, in a rescue experimental setting with near absence of endogenous profilin1 expression, net profilin1/actin and profilin1/polyproline interactions in cells, if at all, were presumably negligible in H119E- and H133S-profilin1 expressers, respectively. Because these two mutants with seemingly normal membrane phosphoinositide interaction in vivo were able to reasonably rescue the phenotypes of profilin1 knockdown cells, phenotypes of R88L-profilin1 expressers likely result from profilin1's reduced interaction with phosphoinositides rather than with actin. However, we do not know whether abolishing any one ligand binding of profilin1 can alter dynamics of its other ligand interactions, possibly through affecting its subcellular localization and/or regulation; thus a certain degree of uncertainty still remains regarding how these profilin1 mutants should behave in cells.

An interesting observation was that profilin1 knockdown increased the sensitivity of MDA-231 cells to lamellipodin depletion. One possibility is that lamellipodin deficiency in parental cells can be compensated by Rap-interacting adaptor molecule (RIAM-1), a lamellipodin homolog that also has a PH domain and binds to profilin1 and Ena/VASP proteins (27). Because RIAM-1 regulates cell adhesion/spreading through actin organization and integrin activation, compensatory action of RIAM-1 might be more pronounced on an adhesion-promoting substrate, such as collage-coated tissue culture substrate used in our motility experiments. If RIAM-induced actin organization at the leading edge, at least, partially requires the involvement of profilin1, cells lacking profilin1 would be expected to be hypersensitive to lamellipodin depletion, as seen in our study.

It was previously reported that phosphoinositide binding of profilin1 can inhibit phospholipase-Cγ (PLCγ)-mediated $PI(4,5)P_2$ hydrolysis in vitro (7, 15). These findings led to a speculation that profilin1 could be a phosphoinositide regulator, but it was never confirmed in vivo. Therefore, our data showing profilin1's negative regulation of $PI(3,4)P_2$ in cells is a unique finding. It is plausible that profilin1 acts as a brake on PI3K-mediated turnover of $PI(4,5)P_2$. For example, profilin1/$PI(4,5)P_2$ interaction may interfere with PI3K's access to $PI(4,5)P_2$, thus effectively down-regulating biosynthesis of $PI(3,4,5)P_3$ and in turn, $PI(3,4)P_2$. Though this can provide at least one mechanistic explanation of how profilin1 regulate lamellipodin distribution at the leading edge, profilin1 could also inhibit membrane targeting of lamellipodin through competition for $PI(3,4)P_2$ binding.

In summary, we have shown in this study that profilin1, generally considered a promigratory molecule, can also inhibit cell motility by suppressing docking of other proteins at the membrane-cytosol interface via a mechanism requiring its phospholipid interaction.

Materials and Methods

Cell Culture, Plasmids/siRNAs, and Transfection. Culture methods of MDA-231 cells, HMEC, and HUVEC have been previously described (9, 12). WT and appropriately mutated (by site-directed mutagenesis) profilin1 were subcloned into EGFP vector (Clontech) with a linker (SGLRSRAQASM) between EGFP and profilin1, and stably transfected in MDA-231 cells using Lipofectamine 2000 (Invitrogen). FP4-mito and AP4-mito constructs were previously described (23). GFP-PTEN and GFP-PH-AKT vectors were generous gifts of Pier Pandolfi (Harvard Medical School, Boston) and Tamas Ballas (National Institutes of Health, Bethesda), respectively. Details of control and profilin1 siRNAs were previously described (11). Lamellipodin siRNA was purchased from Santa Cruz Biotechnology. SiRNAs transfection was performed at 100 nM working concentration (except for profilin1 knockdown in MDA-231 cells, where 50 nM was sufficient) using a custom reagent from Dharmacon, and all experiments were performed 72 h (MDA-231 cells) to 96 h (HMEC, HUVEC) after transfection. For growth-factor treatment, cells were serum starved for 30–40 h before stimulating with either EGF or PDGF (working concentration: 100 ng/mL) for 30 min. For PI3K inhibition, cells were pretreated with 25 μM LY294002 (EMD Bioscience) for 30 min before growth-factor stimulation.

Staining/Image Analyses. General protocols for VASP, lamellipodin, and phalloidin staining have been previously described (11). For $PI(3,4)P_2$ staining, we followed a previous protocol (28). Briefly, cells, fixed/permeabilized by 3.7% formaldehyde/0.1% glutaraldehyde in 0.15 mg/mL saponin solution for 1 h at 37 °C, were stained sequentially with a monoclonal mouse anti-$PI(3,4)P_2$ antibody (Echelon Biosciences; 1:200 dilution in 5% BSA/PBS) for 1 h

and a rhodamine-conjugated secondary antibody for 45 min by standard methods. Fluorescence images of cells, acquired using either Olympus IX71 wide-field (for VASP, lamellipodin, and phalloidin staining) or Olympus FluoView 1000 confocal microscope [for $PI(3,4)P_2$ staining], were background subtracted before intensity analyses. For $PI(3,4)P_2$ quantification, the leading edge was traced and the average fluorescence intensity computed for the traced line was normalized to a similar value calculated for the appropriate control condition. For quantification of lamellipodin staining, the average fluorescence intensity at the leading edge was calculated based on 15–20 line-scan measurements across the lamellipodia, and normalized to the value computed for the appropriate control condition.

Protein Extraction/Immunoblotting. Total cell lysate was extracted with a modified RIPA buffer [50 mM Tris-HCl (pH 7.5), 150 mM NaCl, 1% Nonidet P40, 0.25% sodium deoxycholate, 0.3% SDS, 2 mM EDTA plus protease and phosphatase inhibitors]. For subcellular fractionation, cells were extracted with 0.5% saponin in hypotonic buffer [10 mM Hepes (pH 7.9), 10 mM KCl, 0.1 mM EDTA, 1 mM DTE with protease and phosphatase inhibitors] for 10 min to obtain the cytosolic fraction. Further extraction with 1% Triton X-100 in hypotonic buffer for 15 min followed by clarification of the extract at 18, 000 × *g* for 15 min yielded the membrane fraction. For immunoblotting, all antibodies were used at a 1:1,000 dilution, except those to detect profilin1 (1:500), AKT (1:500), phospho-AKT (1:500), and PDGFR-β (1:300; see Table S2 for detailed antibody information).

F-Actin Estimation. Cellular level of F-actin was estimated using a rhodamine-phalloidin binding assay as previously described (29) (*SI Materials and Methods*). For biochemical verification, Triton-insoluble fraction of cell lysate was prepared and immunoblotted with anti-actin antibody according to our previous protocol (8).

Time-Lapse Cell Motility/Kymography Assay. Time-lapse imaging of single-cell migration and kymograph analyses of net lamellipodial extension have been previously described (11).

Statistics and Data Representation. All statistical tests were performed with ANOVA followed by Newman–Keuls post hoc test for multiple comparisons whenever applicable, and $P < 0.05$ was considered to be statistically significant. In box and whisker plots, dot represents the mean, middle lines of box indicates median, top of the box indicates 75th percentile, bottom of the box measures 25th percentile, and the two whiskers indicate the 10th and 90th percentiles, respectively.

ACKNOWLEDGMENTS. We thank Drs. Richard Bodnar and Ludo Leloup for help with confocal microscopy and phosphoinositide binding assay, respectively. This work was funded by National Institutes of Health Grants CA108607 (to P.R.) and GM58801 (to F.G.).

1. Pollard TD, Borisy GG (2003) Cellular motility driven by assembly and disassembly of actin filaments. *Cell* 112:453–465.
2. Witke W (2004) The role of profilin complexes in cell motility and other cellular processes. *Trends Cell Biol* 14:461–469.
3. Hartwig JH, Chambers KA, Hopcia KL, Kwiatkowski DJ (1989) Association of profilin with filament-free regions of human leukocyte and platelet membranes and reversible membrane binding during platelet activation. *J Cell Biol* 109:1571–1579.
4. Lu PJ, Shieh WR, Rhee SG, Yin HL, Chen CS (1996) Lipid products of phosphoinositide 3-kinase bind human profilin with high affinity. *Biochemistry* 35:14027–14034.
5. Lassing I, Lindberg U (1985) Specific interaction between phosphatidylinositol 4,5-bisphosphate and profilactin. *Nature* 314:472–474.
6. Lambrechts A, Jonckheere V, Dewitte D, Vandekerckhove J, Ampe C (2002) Mutational analysis of human profilin I reveals a second PI(4,5)-P2 binding site neighbouring the poly(L-proline) binding site. *BMC Biochem* 3:12.
7. Goldschmidt-Clermont PJ, Machesky LM, Baldassare JJ, Pollard TD (1990) The actin-binding protein profilin binds to PIP2 and inhibits its hydrolysis by phospholipase C. *Science* 247:1575–1578.
8. Ding Z, Gau D, Deasy B, Wells A, Roy P (2009) Both actin and polyproline interactions of profilin-1 are required for migration, invasion and capillary morphogenesis of vascular endothelial cells. *Exp Cell Res* 315:2963–2973.
9. Ding Z, Lambrechts A, Parepally M, Roy P (2006) Silencing profilin-1 inhibits endothelial cell proliferation, migration and cord morphogenesis. *J Cell Sci* 119: 4127–4137.
10. Janke J, et al. (2000) Suppression of tumorigenicity in breast cancer cells by the microfilament protein profilin 1. *J Exp Med* 191:1675–1686.
11. Bae YH, et al. (2009) Loss of profilin-1 expression enhances breast cancer cell motility by Ena/VASP proteins. *J Cell Physiol* 219:354–364.
12. Zou L, et al. (2007) Profilin-1 is a negative regulator of mammary carcinoma aggressiveness. *Br J Cancer* 97:1361–1371.
13. Roy P, Jacobson K (2004) Overexpression of profilin reduces the migration of invasive breast cancer cells. *Cell Motil Cytoskeleton* 57:84–95.
14. Wu N, et al. (2006) Profilin 1 obtained by proteomic analysis in all-*trans* retinoic acid-treated hepatocarcinoma cell lines is involved in inhibition of cell proliferation and migration. *Proteomics* 6:6095–6106.
15. Sohn RH, Chen J, Koblan KS, Bray PF, Goldschmidt-Clermont PJ (1995) Localization of a binding site for phosphatidylinositol 4,5-bisphosphate on human profilin. *J Biol Chem* 270:21114–21120.
16. Ezezika OC, et al. (2009) Incompatibility with formin Cdc12p prevents human profilin from substituting for fission yeast profilin: Insights from crystal structures of fission yeast profilin. *J Biol Chem* 284:2088–2097.
17. Wittenmayer N, et al. (2004) Tumor suppressor activity of profilin requires a functional actin binding site. *Mol Biol Cell* 15:1600–1608.
18. Wittenmayer N, Rothkegel M, Jockusch BM, Schlüter K (2000) Functional characterization of green fluorescent protein-profilin fusion proteins. *Eur J Biochem* 267:5247–5256.
19. Gau D, Ding Z, Baty C, Roy P (2010) Fluorescence resonance energy transfer (FRET)-based detection of profilin-VASP interaction. *Cell Mol Bioeng*, 10.1007/s12195-010-0133-z.
20. Mimuro H, et al. (2000) Profilin is required for sustaining efficient intra- and intercellular spreading of Shigella flexneri. *J Biol Chem* 275:28893–28901.
21. Krause M, et al. (2004) Lamellipodin, an Ena/VASP ligand, is implicated in the regulation of lamellipodial dynamics. *Dev Cell* 7:571–583.
22. Michael M, Vehlow A, Navarro C, Krause M (2010) c-Abl, Lamellipodin, and Ena/VASP proteins cooperate in dorsal ruffling of fibroblasts and axonal morphogenesis. *Curr Biol* 20:783–791.
23. Bear JE, et al. (2000) Negative regulation of fibroblast motility by Ena/VASP proteins. *Cell* 101:717–728.
24. Smith K, Humphreys D, Hume PJ, Koronakis V (2010) Enteropathogenic *Escherichia coli* recruits the cellular inositol phosphatase SHIP2 to regulate actin-pedestal formation. *Cell Host Microbe* 7:13–24.
25. Goswami S, et al. (2005) Macrophages promote the invasion of breast carcinoma cells via a colony-stimulating factor-1/epidermal growth factor paracrine loop. *Cancer Res* 65:5278–5283.
26. Lu J, Pollard TD (2001) Profilin binding to poly-L-proline and actin monomers along with ability to catalyze actin nucleotide exchange is required for viability of fission yeast. *Mol Biol Cell* 12:1161–1175.
27. Lafuente EM, et al. (2004) RIAM, an Ena/VASP and Profilin ligand, interacts with Rap1-GTP and mediates Rap1-induced adhesion. *Dev Cell* 7:585–595.
28. Yip SC, et al. (2008) Quantification of PtdIns(3,4,5)P(3) dynamics in EGF-stimulated carcinoma cells: A comparison of PH-domain-mediated methods with immunological methods. *Biochem J* 411:441–448.
29. Diakonova M, Bokoch G, Swanson JA (2002) Dynamics of cytoskeletal proteins during Fcgamma receptor-mediated phagocytosis in macrophages. *Mol Biol Cell* 13:402–411.